NOTES AND CORRESPONDENCE

HRDI Observations of Mean Meridional Winds at Solstice

R. S. LIEBERMAN,[a] W. A. ROBINSON,[b] S. J. FRANKE,[c] R. A. VINCENT,[d] J. R. ISLER,[e] D. C. FRITTS,[e] A. H. MANSON,[f] C. E. MEEK,[f] G. J. FRASER,[g] A. FAHRUTDINOVA,[h] W. HOCKING,[i] T. THAYAPARAN,[i] J. MACDOUGALL,[i] K. IGARASHI,[j] T. NAKAMURA,[k] AND T. TSUDA[k]

[a] *Space Physics Research Laboratory, University of Michigan, Ann Arbor, Michigan*
[b] *Department of Atmospheric Sciences, University of Illinois at Urbana–Champagne, Urbana, Illinois*
[c] *Department of Electrical and Computer Engineering, University of Illinois at Urbana–Champagne, Urbana, Illinois*
[d] *Department of Physics and Mathematical Physics, University of Adelaide, Adelaide, Australia*
[e] *Laboratory for Atmospheric and Space Physics, University of Colorado, Boulder, Colorado*
[f] *Institute of Space and Atmospheric Studies, University of Saskatchewan, Saskatoon, Saskatchewan, Canada*
[g] *Department of Physics, University of Canterbury, Christchurch, New Zealand*
[h] *Department of Physics, Kazan State University, Kazan, Russia*
[i] *Department of Physics, University of Western Ontario, London, Ontario, Canada*
[j] *Communication Research Laboratory, Tokyo, Japan*
[k] *Radio Atmospheric Science Center, Kyoto University, Uji, Kyoto, Japan*

4 February 1997 and 2 September 1997

ABSTRACT

High Resolution Doppler Imager (HRDI) measurements of daytime and nighttime winds at 95 km are used to deduce seasonally averaged Eulerian mean meridional winds during six solstice periods. These estimates are compared with seasonally averaged radar meridional winds and with results from dynamical and empirical wind models. HRDI mean meridional winds are directed from the summer pole toward the winter pole over much of the globe. Peak equatorward winds of about 15 m s^{-1} are usually observed in the summer hemisphere near 30°. A local minimum in the equatorward winds is often observed poleward of this latitude, with winds approaching zero or reversing direction. A similar structure is seen in contemporaneous radar winds. This behavior differs from residual meridional wind patterns predicted by models. The discrepancies may be related to gravity wave paramaterizations or a consequence of planetary wave influences.

1. Introduction

Zonally averaged winds and temperatures in the middle atmosphere are far from radiative–photochemical equilibrium (e.g., Andrews et al. 1987). In a pioneering study, Murgatroyd and Singleton (1961) calculated the diabatic heating corresponding to observed zonal mean temperatures and determined the global meridional and vertical winds required to balance this heating. The stratospheric and mesospheric circulation they obtained was thermally direct, characterized by rising motion over the summer pole, sinking motion over the winter pole, and a well-defined meridional flow toward the winter pole. This pattern was consistent with observed distributions of stratospheric water vapor and ozone (Brewer 1949; Dobson 1956). It is now known that this so-called Brewer–Dobson circulation in the middle atmosphere is maintained largely by eddy motions that transfer heat and momentum to the mean flow through nonconservative processes.

The earliest studies of wave-driven circulations (e.g., Leovy 1964) considered perturbations about the conventional Eulerian mean (i.e., the zonally averaged) winds. In practice, it is often difficult to infer the net eddy forcing of the mean flow from the Eulerian mean circulation because of the near-cancellation between the vertical advection of potential temperature by the Eulerian mean vertical velocity and the planetary-wave heat flux divergence. In 1978, Andrews and McIntyre introduced an alternative formalism, the ''transformed Eulerian mean (TEM).'' Within the TEM framework it can be shown (see Andrews et al. 1987) that the zonal mean flow is modified permanently only by nonconservative eddies. In the middle atmosphere, these eddies drive a ''residual'' mean meridional wind directed from the summer pole to the winter pole. In order to satisfy mass continuity, this requires a residual mean rising (sinking) motion in the summer (winter) hemisphere. The residual mean vertical velocity is that portion of the Eulerian mean vertical velocity for which its ad-

Corresponding author address: Dr. Ruth S. Lieberman, Colorado Research Associates, 3380 Mitchell Lane, Boulder, CO 80301.
E-mail: ruth@colorado-research.com

vection of potential temperature is not canceled by the convergence of the meridional eddy heat flux. Rising (sinking) residual motions result in adiabatic cooling (heating) in a stably stratified atmosphere. It is this adiabatic heating and cooling induced by the residual mean vertical motion that prevents the atmosphere from relaxing to temperatures in radiative equilibrium.

In addition to providing a clearer definition of wave-driven circulations, the TEM formalism has another advantage over the conventional Eulerian mean. Dunkerton (1978) showed that in the presence of steady and conservative planetary waves and under quasigeostrophic scaling the residual (or diabatic) circulation is equivalent to the zonally averaged Lagrangian, or mass motion. The TEM framework thus provides a useful tool for quantifying transport in the atmosphere.

The residual mean circulation can be diagnosed from observed or modeled diabatic heating rates and used to infer tracer transport (Garcia and Solomon 1983; Solomon et al. 1986; Stordal et al. 1985; Eluskiewicz et al. 1996) and eddy driving of the mean flow (Gille et al. 1987; Hitchman and Leovy 1986; Shine 1989; Huang and Smith 1991). In the upper mesosphere and lower thermosphere, which are the regions of interest for this paper, gravity waves are believed to play a dominant role in driving the mean winds at midlatitudes. If gravity waves alone drive the circulation, the transformed and the Eulerian representations of the mean flow are nearly equivalent. In reality, there is evidence that the dissipating diurnal tides influence the mean zonal flow in the equatorial lower thermosphere (Lieberman and Hays 1994; Lieberman 1997). Theory predicts that these motions induce a weak two-cell circulation equatorward of 40° in each hemisphere (Miyahara 1984; Miyahara and Wu 1989). Because the meridional heat fluxes associated with the tides are not negligible, they can contribute to a difference between the Eulerian and transformed Eulerian mean circulations. It has also been suggested that the 2-day wave can drive the mean circulation in the midlatitude upper mesosphere during summertime (Plumb et al. 1987; Fritts et al. 1996).

This note presents the global distribution of Eulerian mean meridional winds at 95 km inferred from the *Upper Atmosphere Research Satellite* (*UARS*) High Resolution Doppler Imager (HRDI). Our interest in the Eulerian mean meridional wind derives from the fact that near the equator, and in the midlatitudes at summer solstice, it is likely to approximate the transformed Eulerian mean meridional wind. Results are presented for six periods centered approximately about the solstices, with emphasis upon the flow in the summer hemisphere. The information obtained from this study supplements existing meridional wind climatologies derived largely from mesospheric radar and rocket winds (e. g., Manson et al. 1991; Portnyagin and Solovjova 1992a,b; Hedin et al. 1996). Section 2 outlines the data sources and averaging procedures. HRDI wind fields are presented in section 3 and are compared with radar measurements and empirical wind determinations. The results are discussed and summarized in section 4.

2. Data

HRDI is a triple-etalon Fabry–Perot interferometer/photometer designed to measure winds in the stratosphere, mesosphere, and lower thermosphere. Daytime winds over the range 60–115 km are inferred from the Doppler shift of the O_2 atmospheric band emission features. Line-of-sight wind velocities are measured from two nearly orthogonal directions. A sequential estimator described by Ortland et al. (1995) is used to recover vertical profiles of daytime horizontal winds reported every 2.5 km. This study uses version 10 of level 2 HRDI winds, archived at the University of Michigan Space Physics Research Laboratory. (A gridded, interpolated version of these winds is archived and distributed by Goddard Space Flight Center.) Version 10 winds are smoothed in the vertical using a Gaussian weighting function with an *e*-folding depth of 10 km. At night HRDI senses a narrow O_2 atmospheric band emission layer that generally peaks near 94 ± 2 km, with a Gaussian half-width of 4 km (Burrage et al. 1994; Skinner et al. 1998). As a result, nighttime winds are reported for only one altitude, nominally at 95 km.

HRDI is mounted on the *Upper Atmosphere Research Satellite* and has been operational since October 1991. *UARS* completes about 15 orbits per day, precessing westward at a rate of about 5° longitude per day. Resolution along the orbit track is about 500 km. At a given latitude, each day's measurements generally occur at nearly the same local time, which shifts about 20 minutes forward on consecutive days. Therefore, 36 days of sampling are required in order to collect 18–24 hours of HRDI daytime and nighttime measurements at 95 km. From November 1991 to March 1994 HRDI generally sampled the mesosphere on alternate days. After March 1994 the mesosphere was usually sampled daily, but on alternate orbits. Nighttime winds have been sampled daily since August 1992. Between 2 June and 22 July 1992 HRDI was offline due to problems with the *UARS* solar array. In April 1995 the solar array drive failed altogether, and in consequence HRDI measurements have been severely curtailed.

This study examines winds during six seasons: 20 December 1991–18 February 1992, 4 December 1992–1 February 1993, 12 June–11 August 1993, 11 December 1993–9 February 1994, 13 June–12 August 1994, and 14 December 1994–12 February 1995. For brevity, these are referred to hereafter as ''solstice intervals''; however, we note that the centroid of these intervals lags the actual solstice by one or two weeks. During a given interval, daytime and nighttime meridional winds at 95 km are collected separately each day and averaged in longitude. This procedure results in at least two daily longitudinally averaged mean wind values, obtained at two distinct local times. It should be noted that the

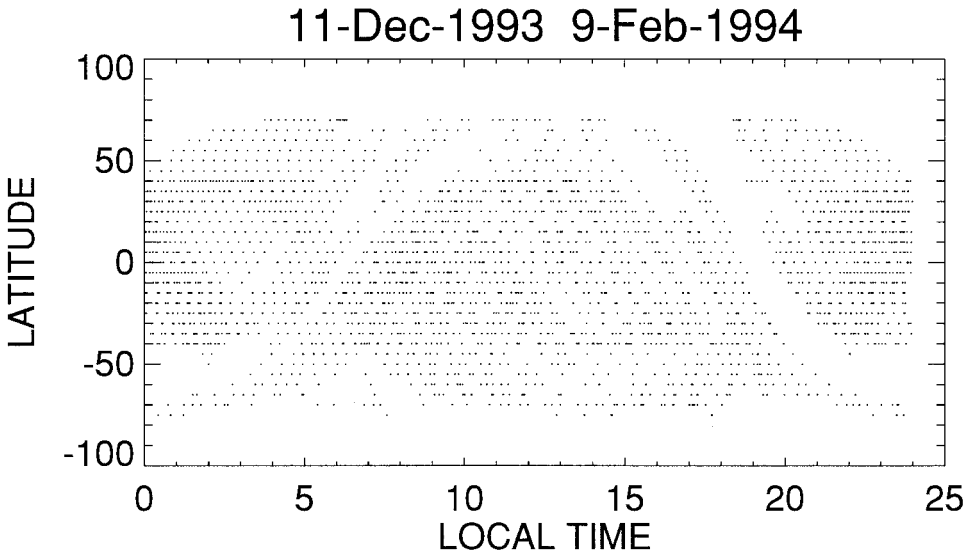

FIG. 1. Latitude distribution of local time coverage during 11 December 1993–9 February 1994.

longitudinal mean obtained at a fixed local time contains the tidal as well as the climatological mean meridional wind (Hays et al. 1994). Figure 1 shows a latitude–local time distribution during a typical 60-day interval, which indicates that about 18–24 hours of local times are sampled over much of the globe. We emphasize that this pattern of local time coverage is restricted to the 95-km level; at all other levels HRDI sampling is confined to daylight hours. Daily longitudinally averaged winds obtained over a 60-day solstice interval are composited by local time, and fit to the mean, 24-h and 12-h harmonics. The time mean (i.e., 60 day) component of the zonally averaged meridional wind is interpreted as the climatological mean meridional wind.

Radar winds at the locations indicated in Table 1 are averaged over the HRDI seasons of interest. Medium frequency (MF) radars (also called partial reflection radars) determine the horizontal drift velocity of weakly ionized irregularities that partially reflect the incident radio waves from the height range 60–100 km. These irregularities are associated with neutral turbulence and related wave processes, and are assumed to drift with the neutral wind (Phillips et al. 1994; Turek et al. 1995). Meteor wind (MW) radars detect echoes due to ionized meteor trails that move with the neutral wind. More complete descriptions of the radar systems indicated in Table 1 can be found elsewhere (e.g., Vincent 1984; Manson et al. 1987; Nakamura et al. 1991; Vincent and Lesicar 1991; Franke and Thorsen 1993; Fritts and Isler 1994; Lysenko et al. 1994; Thayaparan et al. 1995; Tsuda et al. 1995). HRDI and MF radar winds have been extensively compared at Adelaide, Urbana, Christmas Island, Hawaii, Juliusruh (55°N, 13°E), and Saskatoon. At these locations, HRDI and radar wind directions are in agreement, although HRDI magnitudes are systematically larger above 85 km (Burrage et al. 1996). The reasons for this discrepancy are not fully understood. Signal saturation of the MF radar system (Vincent et al. 1994) may account in part for the differences between HRDI and radars; also, it appears that these are rather sensitive to HRDI and radar sampling (S. J. Franke, 1996, personal communication). Comparisons between radar and HRDI climatological mean meridional winds are therefore most useful for validating the sense of the mean meridional flow.

TABLE 1. Coordinates of radar station data used in this study.

Radar site	Location	Attributes
Kazan, Russia	(56°N,49°E)	MW
Saskatoon, Saskatchewan, Canada	(52°N,107°W)	MF
London, Ontario, Canada	(43°N,81°W)	MF
Urbana, Illinois	(40°N,88°W)	MF
Kyoto, Japan	(35°N,136°E)	MW
Yamagawa, Japan	(31°N,132°E)	MF
Kauai, Hawaii	(22°N,160°W)	MF
Christmas Island	(2°N,157°W)	MF
Jakarta, Indonesia	(6°S,107°E)	MW
Adelaide, S Australia	(35°S,138°E)	MF
Christchurch, New Zealand	(44°S,173°E)	MF

3. HRDI and radar winds

Figure 2 shows composite HRDI zonal-mean zonal winds for the two boreal and four austral summer periods considered in this study. Values are plotted only at latitudes where at least 12 daytime hours of winds are sampled in order to minimize the contamination by semidiurnal tides of daytime global wind patterns. The summer hemisphere is characterized by a stratospheric easterly (or westward) jet, which reverses to westerly (eastward) between 85 and 90 km. Peak westerly winds occur in the summer and along an axis tilting poleward

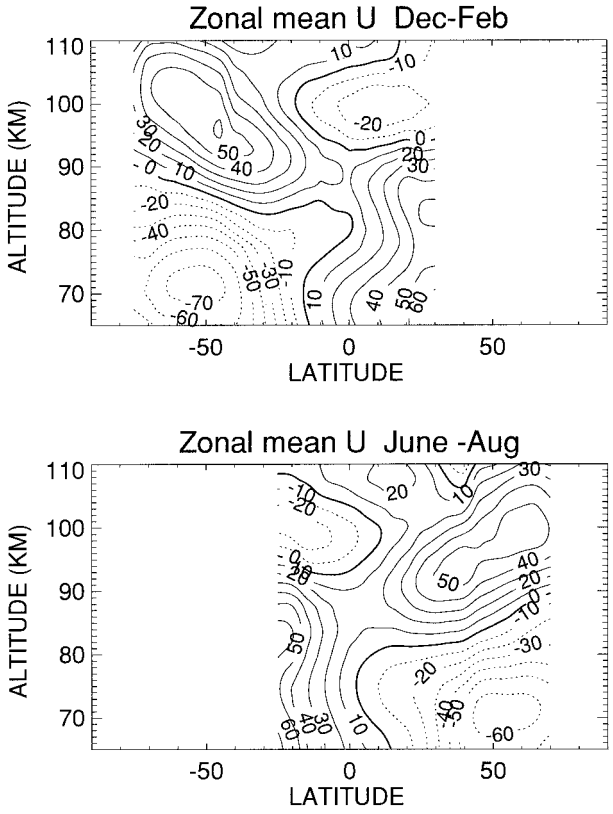

FIG. 2. Composite latitude–height distribution of zonal-mean zonal wind during solstices. Data plotted only at latitudes where at least 12 hours of local time are averaged.

and upward between 90 and 100 km. Thus, poleward of 50° the maximum westerlies occur closer to 100 km, while equatorward of 50° peak westerlies occur closer to 90 km. This pattern differs somewhat from the CIRA-1986 climatology (Fleming et al. 1990) in that the southern summer hemisphere jet reverses between 80 and 85 km, and the maximum mesosphere and lower thermosphere (MLT) westerlies are at 100 km at both austral and boreal summer latitudes. Comparisons of HRDI zonal mean winds with radar zonal wind profiles within each season (not shown) show good agreement in wind direction and level of maximum wind at latitudes poleward of 30°. At these latitudes, however, HRDI zonal mean wind maxima sometimes exceed radar values by more than a factor of 2.

Figure 3 shows HRDI mean meridional winds at 95 km for the six solstice-centered periods considered in this study. Winds are generally directed northward during austral summers and southward during boreal summers. Wind speeds are on the order of 10 m s^{-1}. Peak values range from 15 to 20 m s^{-1} and are observed in the summer hemisphere between 20° and 30°. Poleward of the latitude of the summer maximum, the flow is weaker, and may vanish (11 Dec 1993–9 Feb 1994 and 13 Jun–12 Aug 1994), or reverse direction near 45°–50° (12 Jun–11 Aug 1993). During the solstices of 1993–95, data are available in the summer hemisphere poleward of 50° and indicate that the equatorward component of the wind reintensifies at these higher latitudes.

The mean meridional wind is interpreted as the 18–24-h average of meridional winds sampled over a 60-day duration that have been averaged daily at fixed local times. It has already been noted that the daily zonally averaged meridional wind contains large contributions from the migrating diurnal and semidiurnal tides (see section 2). If tidal amplitudes and phases are stationary over the 60-day sampling period, these components can be filtered from the time mean with 12-h and 24-h harmonic fits in local time. However, systematic and random tidal variations will contribute to a spurious 24-h mean. Estimates of the monthly averaged (1, 1) diurnal meridional wind show that the amplitude of this mode maximizes at equinox and is weakest at solstice (Burrage et al. 1995b; Lieberman 1997). Shorter-term tidal variations on the order of 5–30 days have also been documented (Fahrutdinova and Hutorova 1992; Isler and Fritts 1995; Nakamura et al. 1996). The (1, 1) mode is driven primarily by water vapor insolation absorption (Chapman and Lindzen 1970) and is conceivably prone to day-to-day variability associated with tropospheric water vapor distributions. A semidiurnal tidal wind climatology at 95 km compiled by Burrage et al. (1995a) indicates peak meridional wind amplitudes in the high latitude (poleward of 40°) summer hemisphere. Thus, migrating tidal amplitudes may vary substantially on timescales ranging from 1 day to 6 months.

The effects of tidal variability upon HRDI mean wind analyses are examined by constructing a model of daily tidal variations during each of the six solstice periods under consideration. Monthly mean values of (1, 1) and semidiurnal spectral coefficients are assigned to the midpoints of each calendar month. Daily values are obtained by linearly interpolating the midmonth values and juxtaposing a random daily variation that varies between 0% and 100%. The daily diurnal and semidiurnal fields are sampled during each solstice period in the manner described in section 2, and analyzed for the mean, 24-h, and 12-h components. The time mean winds resulting from the daily varying tides are plotted in Fig. 3 as open circles. The largest contributions are observed during the December 1991–February 1992 and December 1994–February 1995 solstices near 20° and can be traced to strong solstice–equinox (1, 1) variations during those years (Burrage et al. 1995b; Lieberman 1997). The effects of semidiurnal variations are observed poleward of 50° in the summer hemisphere, particularly during June–August 1993 and 1994, and December 1994–February 1995. During the June–August solstices, the tidal bias of the mean wind has a positive maximum value at about 50° and, in 1994, reverses direction at 65°. A similar but reversed pattern occurs in the summer hemisphere during December 1994–February 1995. Although tidal biases are somewhat consistent with the latitudinal changes in the mean meridional winds, their

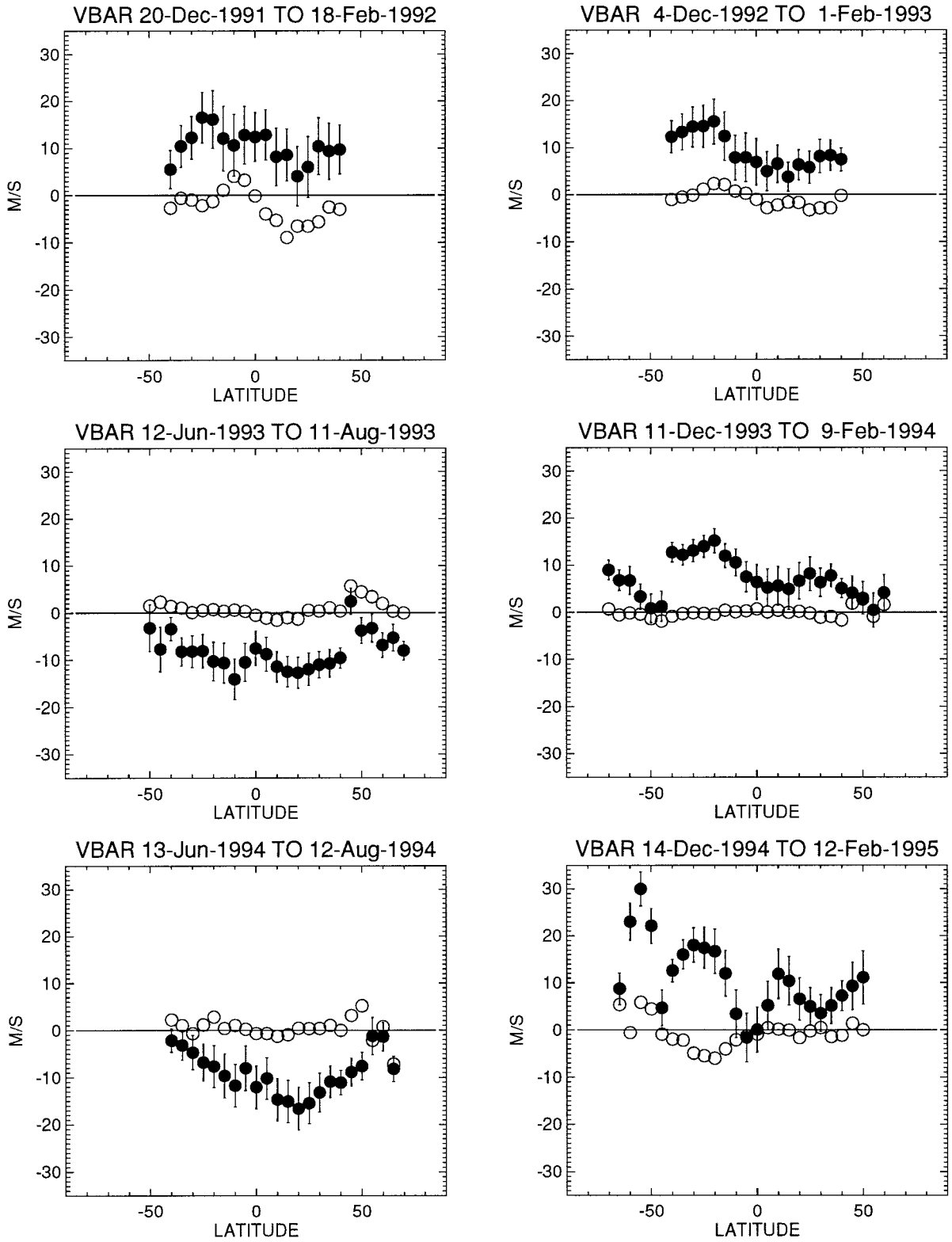

FIG. 3. HRDI Eulerian mean meridional wind at 95 km (filled circles) plotted as a function of latitude. Vertical bars represent 95% confidence limits. Open circles are estimates of spurious component of mean meridional winds induced by daily variations of diurnal and semidiurnal tides.

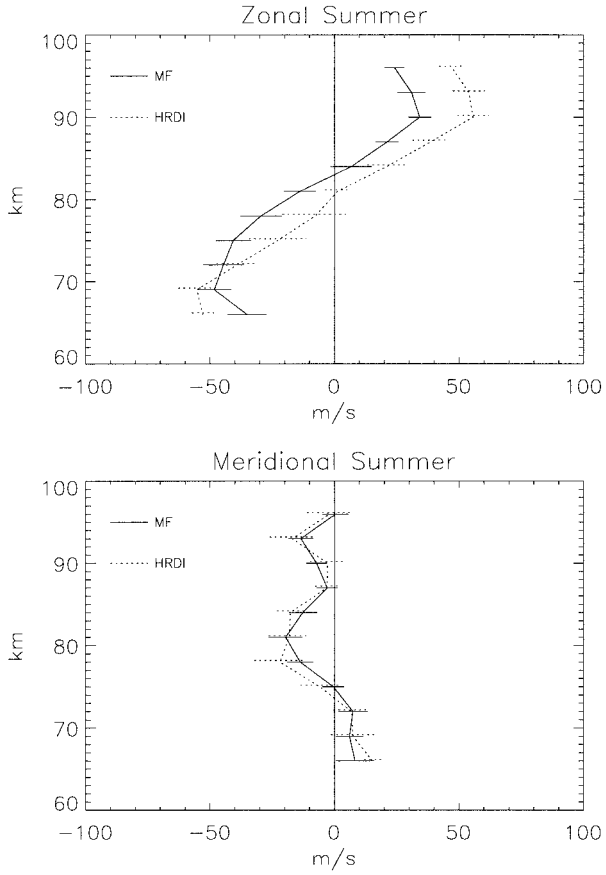

FIG. 4. Averaged coincident HRDI (dotted) and radar (solid) winds at Urbana during June–August of 1992, 1993, and 1994: (a) Zonal wind and (b) meridional wind.

magnitudes are far weaker. We conclude that HRDI seasonal-mean meridional wind determinations are not significantly affected by tidal variations.

HRDI mean meridional winds are compared with radar seasonally averaged winds and with the Hedin et al. (1996) empirical wind model. We focus on the summer season, for which stationary planetary waves are expected to be weak, so that a long time average at a single station is a reasonable proxy for the zonal mean. Radar winds at all stations except Urbana are averaged over the corresponding HRDI observing periods. The Urbana MF radar was offline for much of the HRDI 1993 and 1994 boreal summer study periods due to lightning damage. Comparisons of HRDI and Urbana mean meridional winds are therefore treated somewhat differently.

Figure 4 shows the average values of coincident HRDI and Urbana MF radar winds during the summers of 1992–94. In general, there is very good agreement in the meridonal wind component. (It should be noted that coincident wind measurements reflect the presence of tides and other planetary waves in addition to the long-term mean.) Unfortunately, the paucity of Urbana MF radar measurements during the summers of 1993 and 1994 precludes any credible estimates of the *seasonally* averaged radar mean meridional winds for those summers. Seasonally averaged meridional winds are, however, available at Urbana for the summers of 1995 and 1996 (not shown) and are very similar to each other in both magnitude and direction. We note in Fig. 3 that the main features of the HRDI mean meridional winds at 95 km are repeated during the boreal summers of 1993 and 1994. These include equatorward drift throughout most of the summer hemisphere and the localized weakening or reversal of the flow between 45° and 55°N. Because of the year-to-year repeatability of both HRDI and Urbana mean meridional winds and the close agreement between coincident winds observed by these two platforms, we represent Urbana summer winds of 1993 and 1994 with a composite of the summer winds from 1995 and 1996.

Comparisons of HRDI, radar, and Hedin et al. (1996) mean meridional winds are displayed in Fig. 5. Although HRDI values are derived from meridional winds reported at 95 km, these data represent information spanning the layer 85–105 km with the data nearest 95 km weighted most heavily (see section 2 above, and Fig. 1 of Burrage et al. 1994). For this reason, radar winds at all available levels between 85 and 100 km are included in Fig. 5. It should also be borne in mind that consistency between HRDI and radar wind magnitudes is generally highest at altitudes below 90 km (e.g., Burrage et al. 1996).

During austral summer, radar winds at all levels between 80 and 95 km are directed equatorward in the summer hemisphere. With the exception of December 1994–February 1995, there is little variation with altitude in the intensity of the mean meridional wind. Adelaide meridonal winds at all reported levels are weaker than HRDI 95-km values, while magnitudes at Christchurch are in better agreement with HRDI. During boreal summers, radar winds measured equatorward of 40°N are directed southward at all levels. Poleward of 40°N, radar meridional winds show more vertical variation. At Urbana, composite meridional winds above 86 km are consistently directed northward. At London, Ontario, and Saskatoon, the southward component of the wind decreases monotonically with altitude, reversing direction at Saskatoon at 93 km. The behavior of the radar winds above 90 km in the 40°–50°N latitude belt is consistent with HRDI meridional winds at 95 km, where the southward flow substantially weakens and reverses during 1993. In the case of HRDI, southward flow at 95 km is reestablished poleward of 50°N in 1993 and poleward of 60°N in 1994. Only one radar wind profile from Kazan, Russia (56°N), in 1994 is available for comparison and indicates southward flow throughout the 86–94-km level.

In the winter Northern Hemisphere, radar winds are directed opposite to HRDI winds at levels above 90 km. These strong discrepancies may be due to the presence

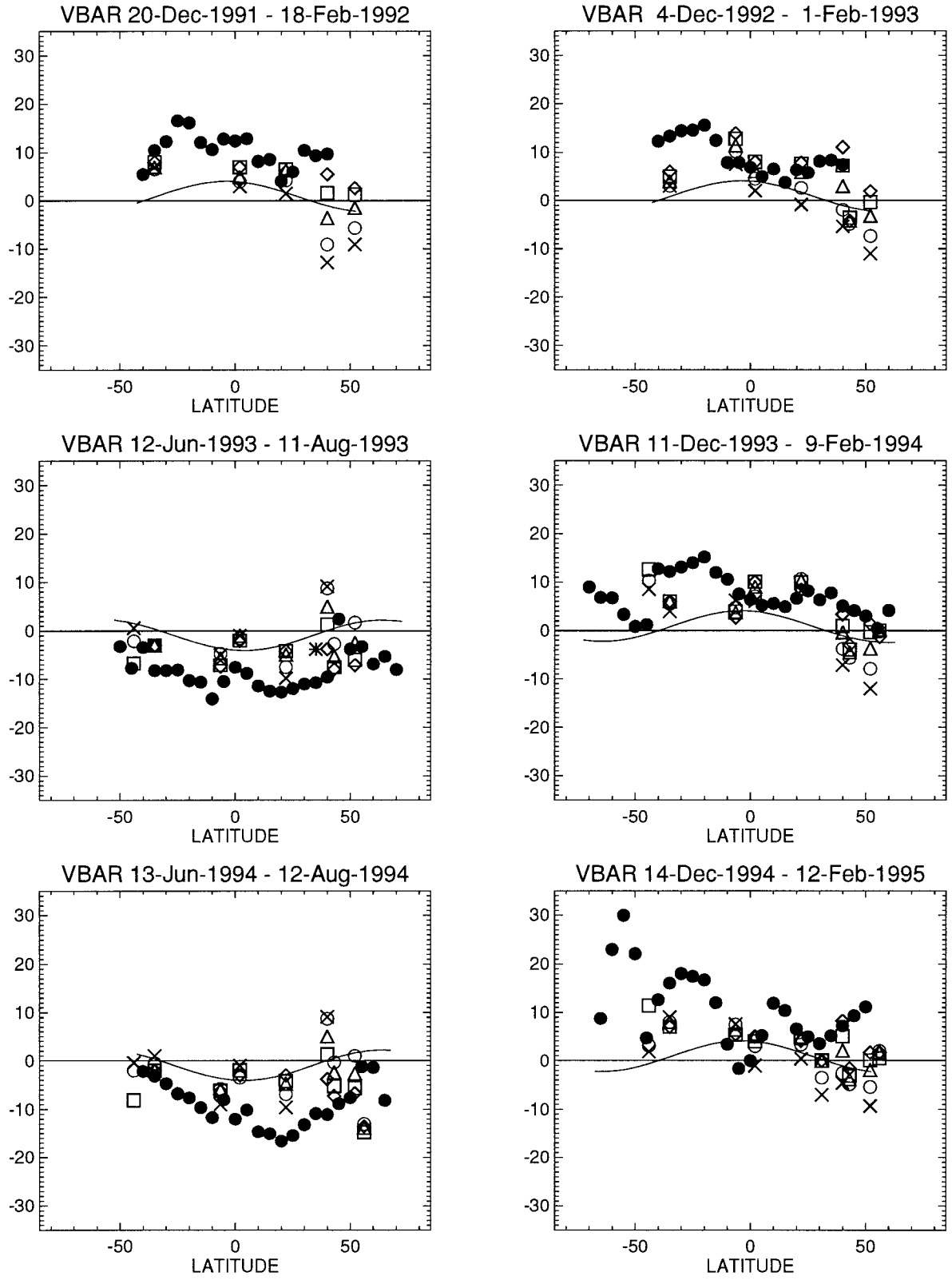

FIG. 5. HRDI $\overline{v}$ at 95 km (filled circles) and radar (symbols) seasonally averaged $\overline{v}$. Solid line indicates values from Hedin et al. (1993) at 95 km. Values plotted at Urbana (40°N) are a composite of winds sampled during June–August of 1995 and 1996 (see text for further discussion). ◇: 85–86 km. □: 88–89 km. Δ: 91–92 km. ○: 93–94 km. *: 95 km. ×: 96–97 km.

of stationary planetary waves, as documented by Manson et al. (1991).

The Hedin et al. (1996) empirical wind model values are derived from incoherent scatter radar, meteor and MF radars, rocket grenade soundings, and gradient winds. At 95 km, the model indicates northward flow between 40°S and 40°N during austral summer and a reverse flow during boreal summer. Peak model winds are observed at the equator. Not surprisingly, this empirical wind climatology shows good general agreement with radar winds in the layer 91–95 km. The pattern differs from HRDI, which shows maximum equatorward flow near 30° in the summer hemisphere and substantially stronger wind magnitudes in general.

4. Discussion and summary

HRDI mean meridional winds at 95 km are directed from the summer hemisphere toward the winter hemisphere, with local reversals near 50° in the summer hemisphere. Similar behavior is observed in seasonally averaged radar meridional winds and in the Hedin climatology that is heavily influenced by radar winds in the mesosphere and lower thermosphere. The observed pattern differs somewhat from recent models of the residual circulation in the MLT. Huang and Smith (1991) used CIRA-86 temperatures together with a radiative transfer model to compute the diabatic heating, which is assumed to balance the advection of potential temperature by the TEM circulation. The residual (or diabatic) circulation they obtained was characterized by a meridionally smooth summer-to-winter-pole flow above 70 km. At 90 km, a local maximum of 6 m s^{-1} appeared in the summer hemisphere near 60° (see Figs. 5a and 6a of Huang and Smith 1991). Inclusion of parameterized thermal effects of gravity wave breaking increased the strength of the maximum residual mean meridional wind to 8 m s^{-1} and produced a second maximum near 20° in the winter hemisphere. These are observed at 85 and 90 km, respectively. Huang and Smith obtained an alternate estimate of the residual mean circulation from the momentum and continuity equations using Lindzen's parameterization for gravity wave stress. The resulting mean meridional wind in December had greater structure in latitude and decreased more rapidly with height in the summer hemisphere above the altitude of the maximum meridional wind (~85 km). In all cases, the modeled meridional winds at 95 km are weaker than those derived from HRDI.

A more recent study by Portmann (1994) determined the residual mean circulation using an updated version of the 1985 Garcia and Solomon model. An improved radiative heating calculation is used together with parameterized gravity wave momentum and thermal forcing. At 95 km, the summer-to-winter-hemisphere flow is nearly uniform; near 90 km there is a local maximum of 20 m s^{-1} in the summer hemisphere at 30°. This is more consistent with HRDI observations, although it does not capture the sharp decrease and near-reversal of the flow observed poleward of 30°. The differences in the meridional structure between the modeled and observed meridional winds may depend on the parameterization of the wave processes that drive the residual circulation. They may also reflect the influence of planetary waves in the upper mesosphere and lower thermosphere, which have not been included in the models. Planetary waves can cause discrepancies between the Eulerian and transformed Eulerian mean circulations. Furthermore, they may contribute additional regions of wave driving of the circulation.

The diurnal and semidiurnal tides are prominent planetary-scale features in the mesosphere and lower thermosphere, which are subjected to breaking or dissipation in the lower thermosphere. Calculations by Portnyagin and Solovjova (1998) show that the mean meridional wind associated with momentum flux divergence of the semidiurnal tide is extremely weak (<2 m s^{-1}) in the summer lower thermosphere. Miyahara (1984) and Miyahara and Wu (1989) calculated the Eulerian mean meridional wind induced by the diurnal tide. This contribution is strongest between 80 and 110 km (about 10 m s^{-1}) but confined equatorward of 40°.

Transient 2-day waves are a recurring feature in the summer hemisphere. Plumb et al. (1987) linked a summertime 2-day wave event at Adelaide to westward and northward accelerations of the prevailing wind. These changes were shown to be consistent with the wave–mean flow interactions predicted by a simple quasi-geostrophic model of transient and dissipating perturbations. A more recent study by Fritts et al. (1996) examined the global structure of 2-day waves and their associated heat and momentum fluxes at 95 km. The acceleration of the prevailing zonal wind was not fully balanced by the latitudinal gradients of the meridional flux of zonal momentum, implying that a mean meridional wind and associated Coriolis torque is required in the zonal momentum budget. A full interpretation of HRDI Eulerian mean winds may therefore require knowledge of the planetary wave spectrum and their spatial heat and momentum flux distributions.

Acknowledgments. This research is supported under NASA Contracts NAS 5-27751 (RSL) and NAG5-2786 (JRI and DCF), and NSF Grants ATM-9523791 (RSL) and ATM-9414177 (JRI and DCF). The UWO MF radar was built by the Canadian Network for Space Research (CNSR) and is also supported by the Natural Sciences and Engineering Research Council (NSERC) of Canada. AHM and CEM acknowledge the support of the University of Saskatchewan (through ISAS) and of NSERC and AES. The Christchurch radar is supported by the University of Canterbury and the New Zealand Foundation for Research, Science and Technology. AF is supported by the Russian Foundation for Basic Research (RFBR) under Grant N 95-IN/RU-989 from the International Association for the Promotion of of Coopera-

tion with Scientists from the New Independent States of the Soviet Union (INTAS). The Jakarta meteor radar is operated under a cooperative agreement with Radio Atmospheric Sciences Center (RASC), Kyoto University, the Indonesian National Institute of Aeronautics and Space (LAPAN), and the Agency for the Assessment and Application of Technology (BPPT), Indonesia.

REFERENCES

Andrews, D. G., and M. E. McIntyre, 1978: Generalized Eliassen–Palm and Charney–Drazin theorems for waves on axisymmetric mean flows and compressible atmospheres. *J. Atmos. Sci.,* **35,** 175–185.

——, J. R. Holton and C. B. Leovy, 1987: *Middle Atmosphere Dynamics.* Academic Press, 489 pp.

Brewer, A. W., 1949: Evidence for a world circulation provided by the measurements of helium and water vapor distribution in the stratosphere. *Quart. J. Roy. Meteor. Soc.,* **75,** 351–363.

Burrage, M. D., N. Arvin, W. R. Skinner, and P. B. Hays, 1994: Observations of the O_2 atmospheric band nightglow by the High Resolution Doppler Imager. *J. Geophys. Res.,* **99,** 15 017–15 023.

——, D. L. Wu, W. R. Skinner, D. A. Ortland, and P. B. Hays, 1995a: Latitudinal and seasonal dependence of the semidiurnal tide observed by the High Resolution Doppler Imager. *J. Geophys. Res.,* **100,** 11 313–11 321.

——, M. E. Hagan, W. R. Skinner, D. L. Wu, and P. B. Hays, 1995b: Long-term variability in the solar diurnal tide observed by HRDI and simulated by the GSWM. *Geophys. Res. Lett.,* **22,** 2641–2644.

——, and Coauthors, 1996: Validation of mesospheric and lower thermospheric winds from the High Resolution Doppler Imager. *J. Geophys. Res.,* **101,** 10 365–10 392.

Chapman, S., and R. S. Lindzen, 1970: *Atmospheric Tides.* Gordon and Breach, 200 pp.

Dobson, G. M. B., 1956: Origin and distribution of the polyatomic molecules in the atmosphere. *Proc. Roy. Soc. London,* **236A,** 187–193.

Dunkerton, T., 1978: On the mean meridional mass motions of the stratosphere and mesosphere. *J. Atmos. Sci.,* **35,** 2325–2333.

Eluskiewicz, J., and Coauthors, 1996: Residual circulation in the stratosphere and lower mesosphere as diagnosed from Microwave Limb Sounder data. *J. Atmos. Sci.,* **53,** 217–240.

Fahrutdinova, A. N., and O. G. Hutorova, 1992: Height-seasonal structure of the wave stream created by longperiod wave disturbances in the lower thermosphere. *Izvestiya,* **28,** 733–738.

Fleming, E. L., S. Chandra, J. J. Barnett, and M. Corney, 1990: Zonal mean temperature, pressure, zonal wind and geopotential height as functions of latitude. *Adv. Space Res.,* **10,** 1211–1259.

Franke, S. J., and D. Thorsen, 1993: Mean winds and tides in the upper middle atmosphere at Urbana (40°N,88°W) during 1991–1992. *J. Geophys. Res.,* **98,** 18 607–18 615.

Fritts, D. C., and J. R. Isler, 1994: Mean motions and tidal and two-day structure and variability in the mesosphere and lower thermosphere over Hawaii. *J. Atmos. Sci.,* **51,** 2145–2164.

——, ——, R. Lieberman, M. D. Burrage, D. R. Marsh, T. Nakamura, T. Tsuda, and R. A. Vincent, 1997: Two-day wave structure, variability, and mean-flow interactions observed by radar and satellite. *J. Geophys. Res.,* in press.

Garcia, R. R., and S. Solomon, 1983: A numerical model of the zonally averaged dynamical and chemical structure of the middle atmosphere. *J. Geophys. Res.,* **88,** 1379–1400.

——, and ——, 1985: The effect of breaking gravity waves on the dynamics and chemical composition of the mesosphere and lower thermosphere. *J. Geophys. Res.,* **90,** 3850–3868.

Gille, J. C., L. V. Lyjak, and A. K. Smith, 1987: The global residual mean circulation in the middle atmosphere for the northern winter period. *J. Atmos. Sci.,* **44,** 1437–1453.

Hays, P. B., and Coauthors, 1994: Observations of the diurnal tide from space. *J. Atmos. Sci.,* **51,** 3077–3093.

Hedin, A. E., and Coauthors, 1996: Empirical wind model for the upper, middle, and lower atmosphere. *J. Atmos. Terr. Phys.,* **58,** 1421–1447.

Hitchman, M. H., and C. B. Leovy, 1986: Evolution of the zonal mean state in the equatorial middle atmosphere during October 1978–May 1979. *J. Atmos. Sci.,* **43,** 3159–3176.

Huang, T. Y. W., and A. K. Smith, 1991: The mesospheric diabatic circulation and the parameterized thermal effect of gravity wave breaking on the circulation. *J. Atmos. Sci.,* **48,** 1093–1111.

Isler, J. R., and D. C. Fritts, 1995: Mean winds and tidal and planetary wave motions over Hawaii during ALOHA-93. *Geophys. Res. Lett.,* **22,** 2821–2824.

Leovy, C. B., 1964: Simple models of thermally driven mesospheric circulation. *J. Atmos. Sci.,* **21,** 327–341.

Lieberman, R. S., 1996: Long-term variations of zonal mean winds and (1,1) driving in the equatorial lower thermosphere. *J. Atmos. and Solar-Terr. Phys.,* **59,** 1483–1490.

——, and P. B Hays, 1994: An estimate of the momentum deposition in the lower thermosphere by the observed diurnal tide. *J. Atmos. Sci.,* **51,** 3094–3105.

Lysenko, I. A., Y. I. Portnyagin, A. N. Fahrutdinova, R. A. Ishmuratov, A. H. Manson, and C. E. Meek, 1994: Wind regime at 80–110 km at mid-latitudes of the northern hemisphere. *J. Atmos. Terr. Phys.,* **56,** 31–42.

Manson, A. H., C. E. Meek, M. Massebeuf, and J. L. Fellous, 1987: Mean winds of the upper middle atmosphere (~70–110 km) from the global radar network: Comparisons with CIRA 72 and new rocket and satellite data. *Adv. Space Res.,* **7,** 143–153.

——, and Coauthors, 1991: Comparisons between satellite-derived gradient winds and radar-derived winds from the CIRA-86. *J. Atmos. Sci.,* **48,** 411–428.

Miyahara, S., 1984: Zonal mean winds induced by solar diurnal tides in the lower thermosphere for a solstice condition. *Dynamics of the Middle Atmosphere,* J. R. Holton and T. Matsuno, Eds., Terra Scientific Publishing, 181–197.

——, and D. H. Wu, 1989: Effects of solar tides on the zonal mean circulation in the lower thermosphere: Solstice condition. *J. Atmos. Terr. Phys.,* **51,** 635–647.

Murgatroyd, R. J., and F. Singleton, 1961: Possible meridional circulations in the stratosphere and mesosphere. *Quart. J. Roy. Meteor. Soc.,* **87,** 125–135.

Nakamura, T., T. Tsuda, M. Tsutsumi, K, Kita, T. Uehara, S. Kato, and S. Fukao, 1991: Meteor wind observations with the Kyoto MU radar. *Radio Sci.,* **26,** 857–869.

——, D. C. Fritts, J. R. Isler, T. Tsuda, R. A. Vincent, and I. M. Reid, 1997: Short-period fluctuations of the diurnal tide observed with low-latitude MF and Meteor radars during CADRE: Evidence for gravity wave/tidal interactions. *J. Geophys. Res.,* **102,** 26 225–26 328.

Ortland, D. A., P. B. Hays, W. R. Skinner, V. J. Abreu, J.-H. Yee, M. D. Burrage, A. R. Marshall, and D. A. Gell, 1995: A sequential estimation technique for recovering atmospheric data from orbiting satellites. *The Upper Mesosphere and Lower Thermosphere: A Review of Experiment and Theory, Geophys. Monogr.,* No. 87, Amer. Geophys. Soc., 329–337.

Phillips, A., A. H. Manson, C. E. Meek, and E. J. Llewellyn, 1994: Long-term comparison of middle atmosphere winds measured at Saskatoon (52°N, 107°W) by a medium-frequency radar and a Fabry–Perot interferometer. *J. Geophys. Res.,* **99,** 12 923–12 935.

Plumb, R. A., R. A. Vincent, and R. L. Craig, 1987: The quasi-two-day wave event of January 1984 and its impact on the mean mesospheric circulation. *J. Atmos. Sci.,* **44,** 3030–3036.

Portmann, R. W., 1994: The heat budget and global change in the mesosphere. Ph.D. thesis, University of Colorado, 187 pp.

Portnyagin, Y. I., and T. V. Solovjova, 1992a: An empirical model of the meridional wind in the mesopause-lower thermosphere,

Part I: A monthly mean model. *Russ. J. Meteor. Hydrol.,* **10,** 28–35.

——, and ——, 1992b: An empirical model of the meridional wind in the mesopause-lower thermosphere, Part II: Height-latitude features of basic components of meridional wind seasonal variations. *Russ. J. Meteor. Hydrol.,* **11,** 29–36.

——, and ——, 1998: On the momentum balance in the lower thermosphere. *Adv. Space Res.,* in press.

Shine, K., 1989: Sources and sinks of zonal momentum in the middle atmosphere diagnosed using the diabatic circulation. *Quart. J. Roy. Meteor. Soc.,* **115,** 265–292.

Skinner, W. R., J.-H. Yee, P. B. Hays, and M. D. Burrage, 1998: Seasonal and local time variations in the O(^{1}S) green line, O_2 atmospheric band, and OH Meinel band emissions as measured by the High Resolution Doppler Imager. *Adv. Space Res.,* in press.

Solomon, S., J. T. Kiehl, R. R. Garcia, and W. Grose, 1986: Tracer transport by the diabatic circulation deduced from satellite observations. *J. Atmos. Sci.,* **43,** 1603–1617.

Stordal, F., I. S. A. Isaksen, and K. Horntveith, 1985: A diabatic circulation two-dimensional model with photochemistry: Simulations of ozone and long-lived tracers with surface sources. *J. Geophys. Res.,* **90,** 5757–5776.

Thayaparan, T., W. K. Hocking, and J. MacDougall, 1995: Middle atmospheric winds and tides over London, Canada (43°N, 81°W) during 1992–1993. *Radio Sci.,* **30,** 1293–1309.

Tsuda, T., and Coauthors, 1995: A preliminary report on observations of equatorial dynamics in Indonesia with radars and radiosondes. *J. Meteor. Soc. Japan,* **73,** 393–406.

Turek, R. S., K. L. Miller, R. G. Roper, and I. W. Brosnahan, 1995: Mesospheric wind studies during AIDA Act '89: Morphology and comparison of various techniques. *J. Atmos. Terr. Phys.,* **57,** 1321–1343.

Vincent, R. A., 1984: MF/HF radar measurements of the dynamics of the mesopause region—A review. *J. Atmos. Terr. Phys.,* **46,** 961–974.

——, and D. Lesicar, 1991: Dynamics of the equatorial mesosphere: First results with a new generation partial reflection radar. *Geophys. Res. Lett.,* **18,** 825–828.

——, D. A. Holsworth, I. M. Reid, and M. A. Cervera, 1994: Space-antenna wind measurements: The effects of signal saturation. *Wind Observations in the Middle Atmosphere,* M. Geller, Ed., Cent. Natl. d'Etud. Spatiales.